むかわ町穂別博物館研究報告第 32 号（2017 年 3 月）7-41 頁
The Bulletin of the Hobetsu Museum, no.32 (Mar., 2017), p.7–41.

An early Maastrichtian (latest Cretaceous) ammonoid fauna from the Soya Hill area, Hokkaido, northern Japan

YASUNARI SHIGETA[1], MASATAKA IZUKURA[2] and YUKIYASU TSUTSUMI[1]

[1]*Department of Geology and Paleontology, National Museum of Nature and Science, 4-1-1 Amakubo, Tsukuba, Ibaraki, 305-0005, Japan (e-mail: shigeta@kahaku.go.jp) (e-mail: ytsutsu@kahaku.go.jp)*
[2]*N28 E21-1-3 Higashi-ku, Sapporo, Hokkaido 065-0028, Japan (e-mail: masataka.izukura@apricot.ocn.ne.jp)*

Abstract

An early Maastrichtian (latest Cretaceous) ammonoid fauna is reported from the middle part of the Etanpakku Formation of the Yezo Group exposed along the Onishibetsu and Sarukotsu rivers in the Soya Hill area, northernmost Hokkaido, northern Japan. The fauna comprises nine ammonoid species belonging to eight genera: *Neophylloceras hetonaiense* Matsumoto, *Tetragonites popetensis* Yabe, *T. terminus* Shigeta, *Gaudryceras izumiense* Matsumoto and Morozumi, *Anagaudryceras matsumotoi* Morozumi, *Pachydiscus* sp., *Diplomoceras* sp., *Nostoceras* sp. and *Baculites regina* Obata and Matsumoto. The fauna correlates with the lower part of the *Gaudryceras izumiense* Zone of the upper lower Maastrichtian in the Izumi Group of Southwest Japan. Zircon geochronology also reveals that the ages of the tuffs from the lowest and uppermost parts of the Etanpakku Formation in the Soya Hill area are 72.6±1.6 Ma and 70.6±1.2 Ma, respectively, which infer a late Campanian to earliest middle Maastrichtian age.

Key wards: ammonoid, Cretaceous, Hokkaido, Maastrichtian, Soya Hill
(Recieved 1 October 2016)

Introduction

Strata of the Campanian–Maastrichtian Yezo Group are widely distributed in northernmost Hokkaido (Osanai *et al*., 1959; Matsushita *et al*., 1964; Takahashi and Ishiyama, 1968; Matsumoto and Ohara, 1971). Cape Soya at the northernmost point of Hokkaido has been a classic locality for Campanian ammonoid research since the early work of Jimbo (1894). Matsumoto and Miyauchi (1984) described 30 ammonoid species from the western coastal area of the cape, and Matsumoto (1984b) established a biostratigraphic scheme for the Campanian of Hokkaido. Although Ando and Ando (2002) reported the occurrence of several ammonoid specimens of probable Maastrichtian age from the Soya Hill area, ammonoids representative of this particular stage have not well been studied in northernmost Hokkaido.

To ensure precise stratigraphic attribution of Maastrichtian ammonoids in northernmost Hokkaido, field expeditions were carried out by the authors (Y. S. and M. I.) in 2015 along the Onishibetsu and Sarukotsu rivers in the Soya Hill area (Figure 1). We discovered an early Maastrichtian ammonoid fauna including *Gaudryceras izumiense* Matsumoto and Morozumi, 1980 and *Baculites regina* Obata and Matsumoto, 1963, which are common to the Izumi Group in Southwest Japan. In this paper, we document the fauna and discuss its biostratigraphic implications. We also provide a zircon-based geochronology of the Etanpakku Formation based on its intercalated tuffs.

Outline of stratigraphy

The Yezo Group along the upper course of the Onishibetsu and Sarukotsu rivers can be divided into two units, the Karibetsu and Etanpakku formations in ascending order, as defined by Matsushita *et al*. (1964). These strata are cut and displaced by two major faults striking NNW–SSE (Figures 2, 3). The Karibetsu Formation, consisting of mudstone and sandy mudstone, is mainly exposed in the western part of the area, whereas the Etanpakku Formation, which is composed of various types of sandstone as well as sandy mudstone and conglomerate, is distributed in the middle part of the area between the two major faults.

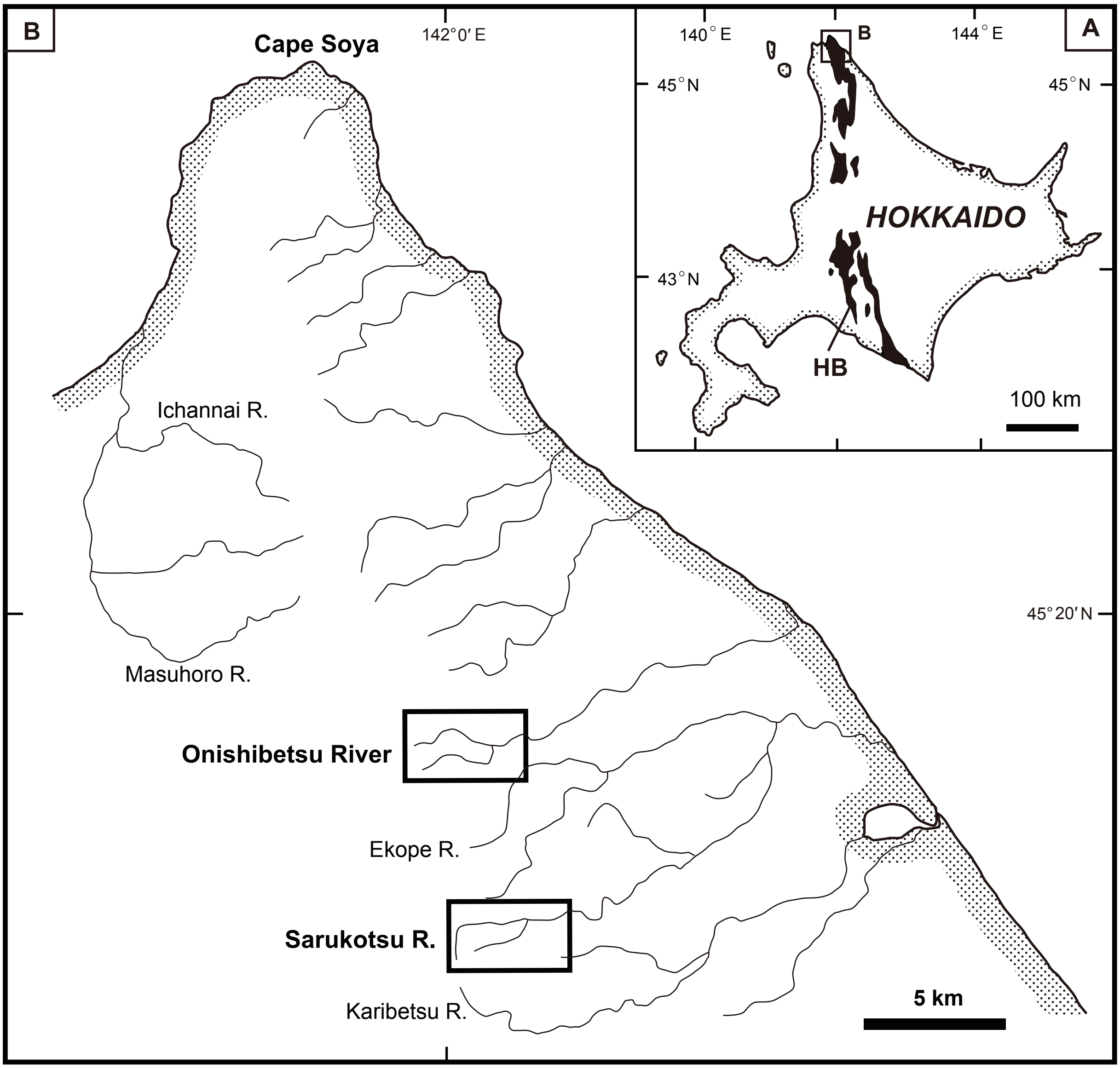

Figure 1. Index maps showing distribution of Yezo Group (black areas) in Hokkaido (**A**) and the studied areas in the Soya Hill area (**B**). HB, Hobetsu.

The Etanpakku Formation is in fault contact with the Karibetsu Formation in the western part and with the Miocene Soya Formation in the eastern part of the area.

The structure in the middle part of the area in the upper course of the Onishibetsu River between the two major faults consists of an anticline with strata on the western limb striking N5–10° westward and dipping 10–30° westward, while beds of the eastern limb strike N20–30° westward and dip 10–30° eastward. In contrast, the structure in the upper course of the Sarukotsu River area consists of a syncline with strata on the northern limb striking N50–60° westward and dipping 10–20° southward, while those of the southern limb strike N30–40° eastward and dip 10–20° northward.

Karibetsu Formation

The Karibetsu Formation is equivalent to the Orannai Formation in the Cape Soya area (Osanai *et al*., 1959) and the Kamikoma Formation in the Nakatonbetsu area (Osanai *et al*., 1963), which is located approximately 40 km southeast of the Soya Hill area.

Exposure.—Uppermost course of the Onishibetsu and Sarukotsu rivers, and middle course of the Rokugousen River, a tributary of the Onishibetsu River (Figures 2, 3).

Thickness.—Greater than 25 m in the Rokugousen River section.

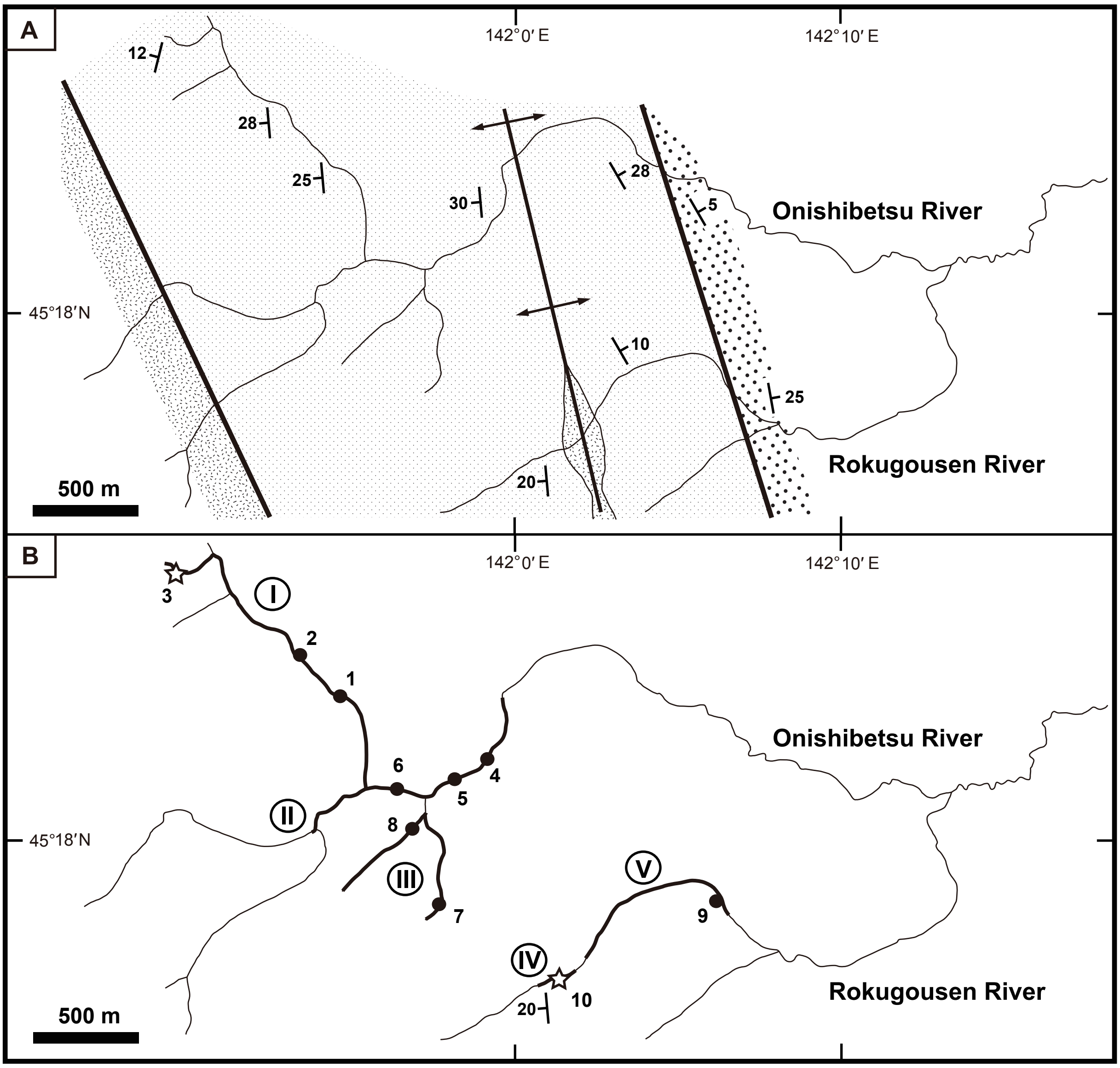

Figure 2. Geological map (**A**) and locality map (**B**) showing study sections (I through V) and fossil localities along the Onishibetsu River and its tributaries in the Soya Hill area, Hokkaido. See Figure 3 for legend.

Stratigraphic relationship.—The Karibetsu Formation is conformably overlain by the Etanpakku Formation. The uppermost part is exposed along the axis of an anticline in the Rokugousen River section, but the stratigraphic position of the formation's outcrops in the uppermost course of the Onishibetsu and Sarukotsu rivers is uncertain.

Lithology.—The formation consists of dark grey, massive mudstone (Figure 4), but detailed sedimentological features are uncertain because of poor exposures.

Fossils.—Although a few calcareous concretions were observed in the mudstone, the formation has not yet yielded megafossils.

Etanpakku Formation

The Etanpakku Formation is equivalent to the Heitarouzawa Formation in the Nakatonbetsu area (Osanai *et al.*, 1963).

Exposure.—Upper course of the Onishibetsu and Sarukotsu rivers and their tributaries (Figures 2, 3).

Thickness.—Greater than 600 m.

Stratigraphic relationship.—The Etanpakku Formation conformably overlies the Karibetsu Formation, but its top portion is in fault contact with the Karibetsu Formation in the uppermost course of the Onishibetsu River.

Lithology.— The lower part of the formation (200-m thick) consists of gray to greenish gray, fine-grained, bedded or massive sandstone intercalated with a 3-m

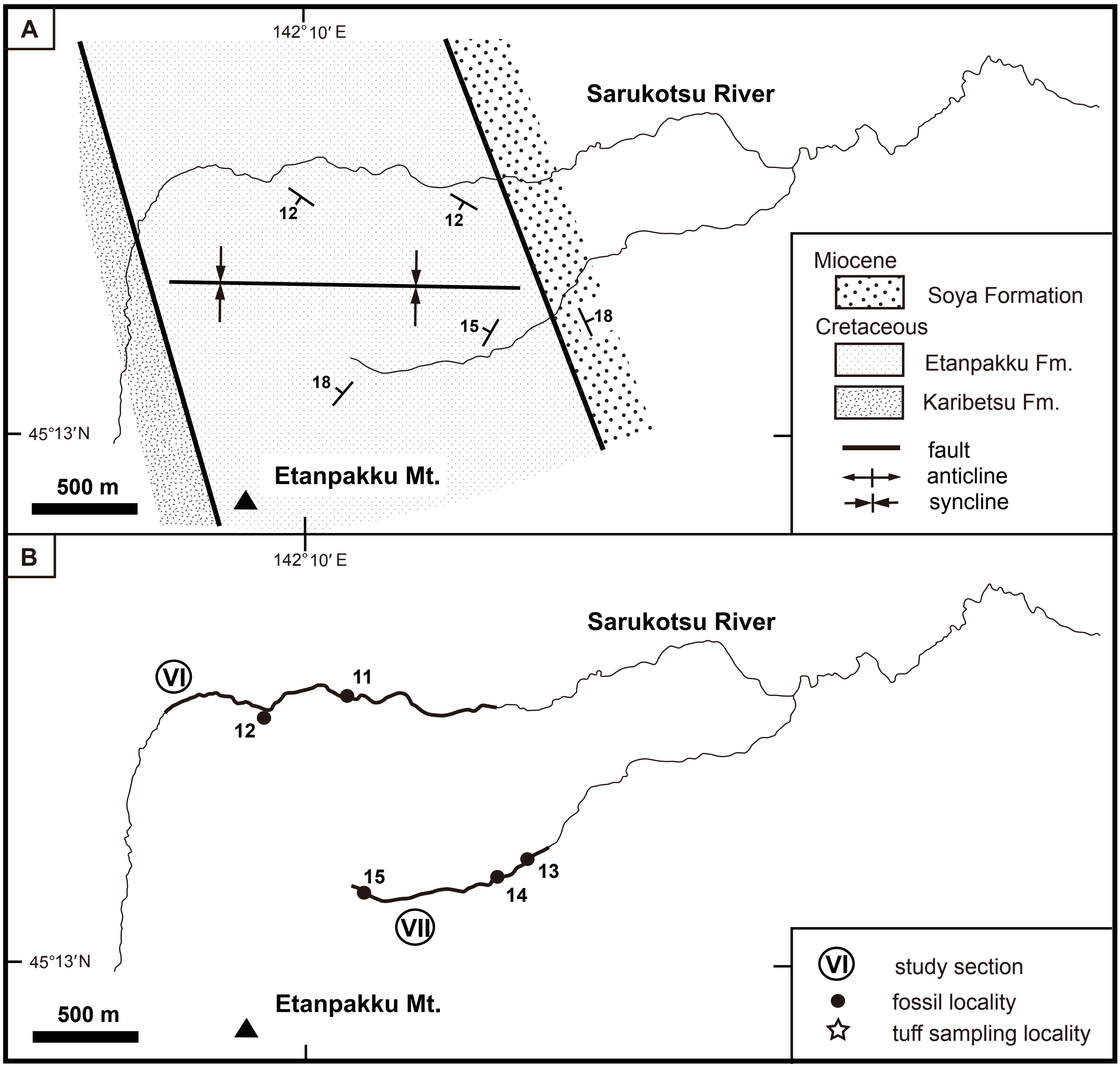

Figure 3. Geological map (**A**) and locality map (**B**) showing study sections (VI, VII) and fossil localities along the Sarukotsu River and its tributary in the Soya Hill area, Hokkaido.

thick white, vitric tuff bed and alternating beds of coarse-grained sandstone and conglomerate composed mainly of rounded to subrounded pebbles and cobbles in greenish gray, medium- to course-grained sandstone matrix (Figure 4).

The middle part of the formation (250-m thick) consists of gray to greenish gray, fine- to course-grained, bedded or massive sandstone in association with dark gray, intensely bioturbated muddy sandstone and sandy mudstone beds (Figure 4). Spherical calcareous concretions containing ammonoids, bivalves and gastropods are common in the muddy sandstone.

The upper part of the formation (150-m thick) also consists of gray to greenish gray, fine- to course-grained, bedded or massive sandstone (Figure 4), but some of the sandstone beds are characterized by low-angle, hummocky cross-stratification. A 2–3-m thick white, vitric tuff bed is intercalated in the uppermost part.

Fossils.—From the lower part of the formation, inoceramid bivalves were collected from the alternating beds of coarse-grained sandstone and conglomerate and fine-grained, massive sandstone (Figures 5, 7A–C).

The muddy sandstone in the middle part of the formation is fossiliferous and inoceramid bivalves (Figures 5, 6, 7D–S, 8) as well as the following ammonoids were collected from calcareous concretions (Figures 5, 6, 12–24): *Neophylloceras hetonaiense*

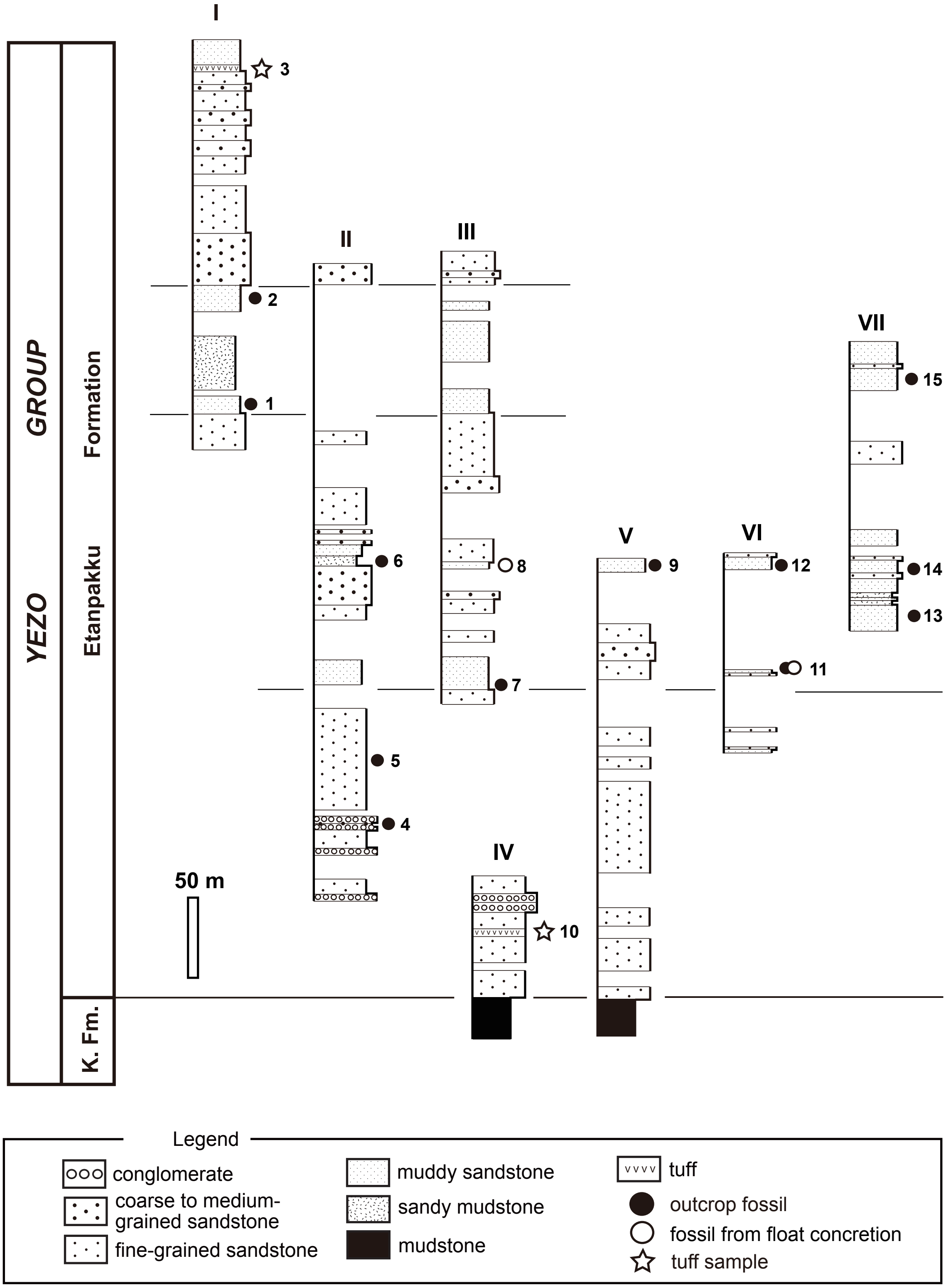

Figure 4. Columnar sections showing localities from which fossils and tuff samples were collected in the Soya Hill area, Hokkaido.

Matsumoto, 1942a, *Tetragonites popetensis* Yabe, 1903, *T. terminus* Shigeta, 1989, *Gaudryceras izumiense* Matsumoto and Morozumi, 1980, *Anagaudryceras matsumotoi* Morozumi, 1985, *Pachydiscus* sp., *Baculites regina* Obata and Matsumoto, 1963, *Diplomoceras* sp. and *Nostoceras* sp.

No fossils were found in the upper part of the formation.

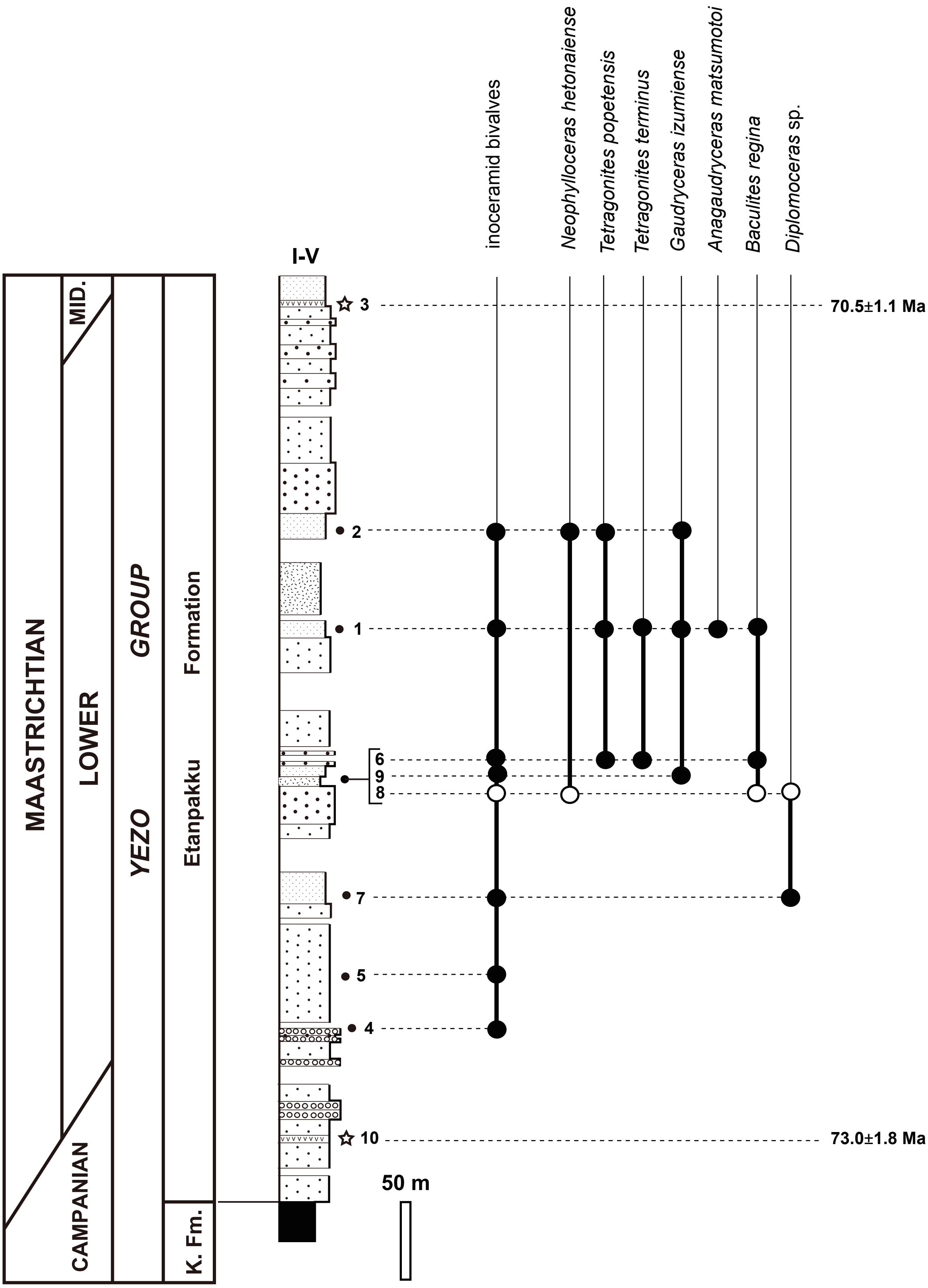

Figure 5. Stratigraphic occurrence of ammonoids and inoceramid bivalves, and U–Pb zircon ages of tuffs in the Etanpakku Formation along the Onishibetsu River and its tributaries in the Soya Hill area, Hokkaido.

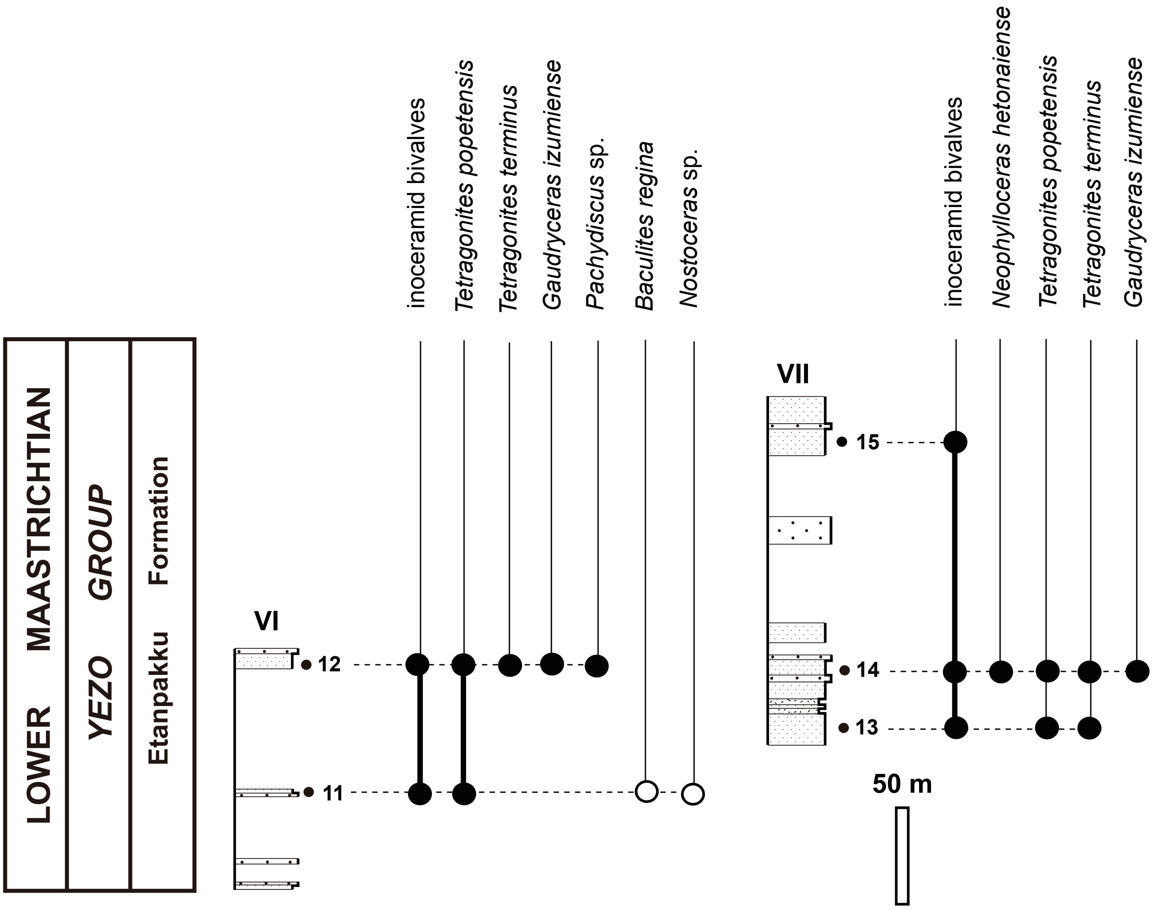

Figure 6. Stratigraphic occurrence of ammonoids and inoceramid bivalves in the Etanpakku Formation along the Sarukotsu River and its tributary in the Soya Hill area, Hokkaido.

Radiometric ages of zircons in tuffs

Material.—Two tuff samples from the Etanpakku Formation were examined for zircon-based radiometric age analyses. The first sample, taken at Loc. 10, was collected from a 2–3-m thick white, vitric tuff bed intercalated in the lowest part of the formation. The other sample, taken at Loc. 3, was collected from a 2–3-m thick white, vitric tuff bed intercalated in the uppermost part of the formation.

Method.—Zircon grains were extracted by standard techniques: crushing, heavy liquid separation and handpicking. Then, the zircon grains, the zircon standard TEMORA2 (^{206}Pb/^{238}U = 0.06679; Black *et al.*, 2004), and the glass standard SRM610 were mounted in epoxy resin and polished until the surface was flat with the center of each grain exposed. Images of both the backscattered electron and cathodoluminescence of the zircon grains were used to select the sites for analysis. U–Pb dating of these samples was carried out using LA-ICP-MS, which was performed on an instrument consisting of a NWR213 laser ablation system (Electro Scientific Industries) and an Agilent 7700x quadrupole ICP-MS (Agilent Technologies) that is installed at the National Museum of Nature and Science at Tsukuba, Japan. The experimental conditions and procedures for the measurements were based on the methods described in Tsutsumi *et al*. (2012). The spot size of the laser was 25 µm. Corrections for common Pb was made on the basis of the measured ^{207}Pb/^{206}Pb ratio or ^{208}Pb/^{206}Pb and Th/U ratios (e.g. Williams, 1998) as well as the model for common Pb compositions proposed by Stacey and Kramers (1975). In this paper, we adopt the ^{207}Pb correction for age discussion because it is more effective in calculating the Phanerozoic ^{238}U–^{206}Pb* age than the ^{208}Pb correction (e.g. Williams, 1998). The pooled ages presented in this study were calculated using Isoplot/Ex software (Ludwig, 2003). The uncertainties in the mean ^{238}U–^{206}Pb* ages represent 95% confidence intervals (95% conf.). ^{206}Pb* indicates

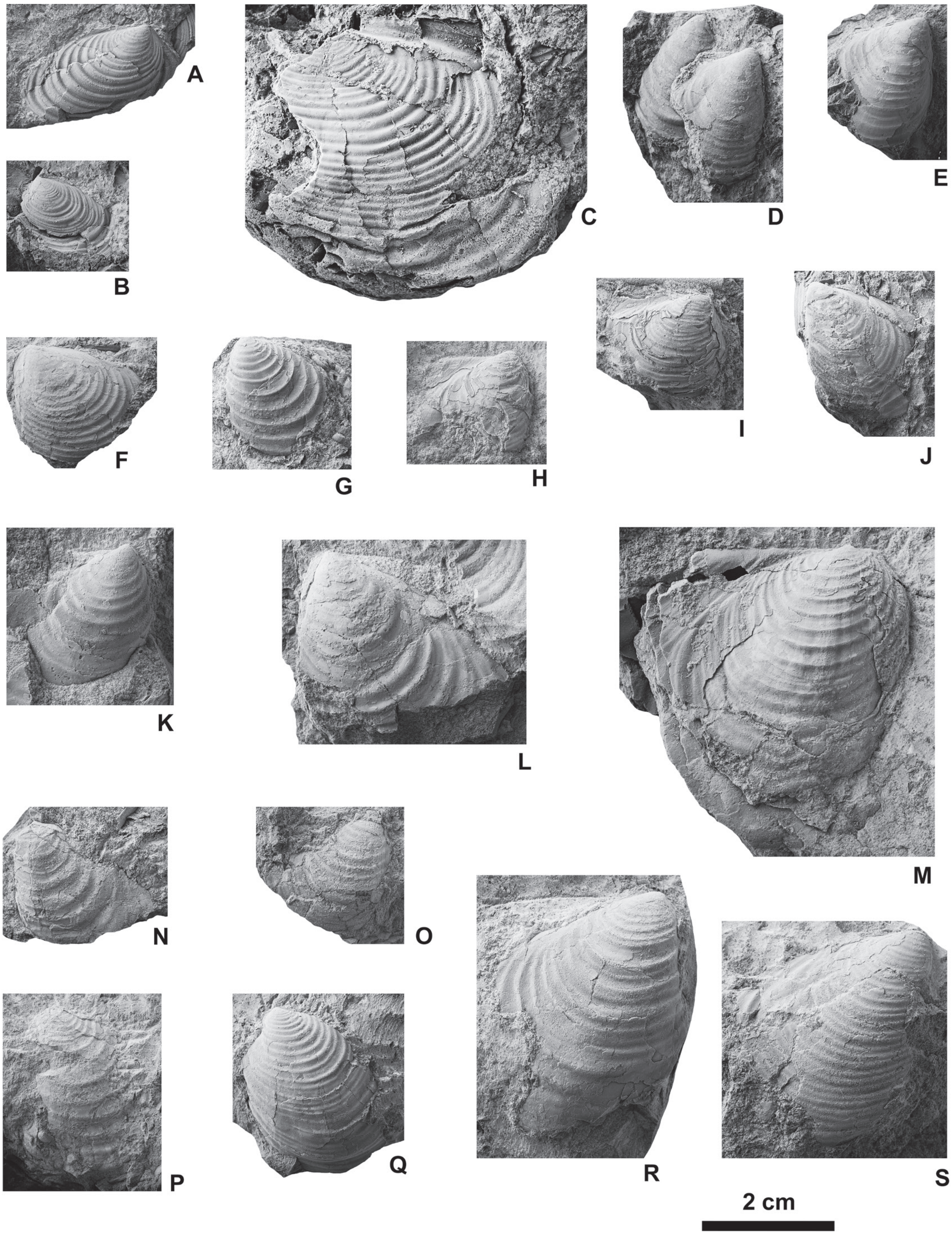

Figure 7. Inoceramid bivalves from the Etanpakku Formation. **A,** HMG-1755 from Loc. 4; **B,** HMG-1756 from Loc. 4; **C,** HMG-1757 from Loc. 5; **D, E,** HMG-1758, 1759 from a float calcareous concretion found near Loc. 8; **F, G,** HMG-1760, 1761 from a float calcareous concretion found near Loc. 8; **H–L,** HMG-1762–1766 from Loc. 6; **M,** HMG-1767 from Loc. 9; **N–P,** HMG-1768–1770 from Loc. 1; **Q,** HMG-1771 from a float calcareous concretion found near Loc. 1; **R, S,** HMG-1772, 1773 from a float calcareous concretion found near Loc. 1.

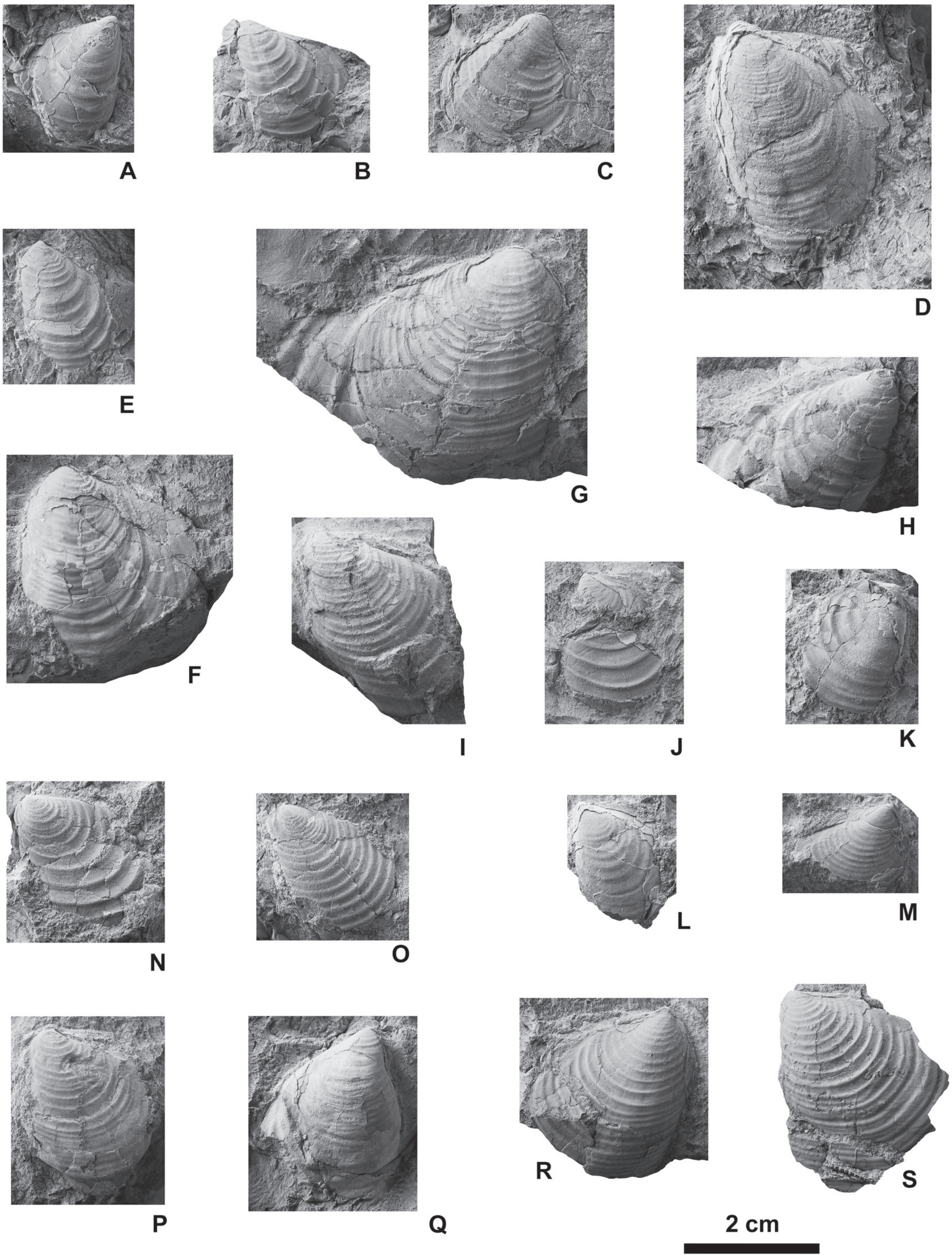

Figure 8. Inoceramid bivalves from the Etanpakku Formation. **A–F,** HMG-1774–1779 from Loc. 2; **G,** HMG-1780 from a float calcareous concretion found near Loc. 2; **H,** HMG-1781 from a float calcareous concretion found near Loc. 2; **I,** HMG-1782 from Loc. 11; **J–M,** HMG-1783–1786 from Loc. 12; **N, O,** HMG-1787, 1788 from a float calcareous concretion found near Loc. 14; **P,** HMG-1789 from a float calcareous concretion found near Loc. 14; **Q,** HMG-1790 from Loc. 13; **R, S,** HMG-1791, 1792 from Loc. 15.

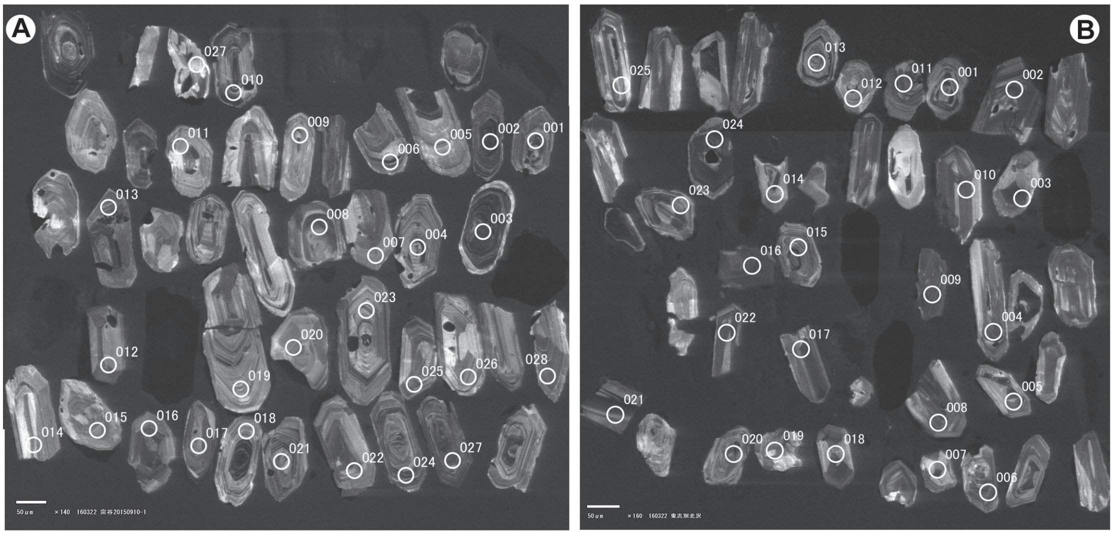

Figure 9. Cathodoluminescence image (CL) of zircon grains from the tuff samples collected at loc. 10 (**A**) and Loc. 3 (**B**). Circles on the grain represent spots analyzed by LA-ICP-MS. Spots are 25 μm across.

radiometric ^{206}Pb.

U–Pb zircon age.—Zircon data in terms of the fraction of common ^{206}Pb, U, and Th concentrations, Th/U, ^{238}U/^{206}Pb*, and ^{207}Pb*/^{206}Pb* ratios, and radiometric ^{238}U/^{206}Pb* ages are listed in Appendix 1. All errors are 1 sigma level. All zircons in the samples show rhythmic oscillatory and/or sector zoning on cathodoluminescence images (Figure 9), which is commonly observed in igneous zircons (e.g. Corfu *et al*., 2003), and their higher Th/U ratios (> 0.1) also support their igneous origin (Williams and Claesson, 1987; Schiøtte *et al*., 1988; Kinny *et al*., 1990; Hoskin and Black, 2000). Figure 10 shows Tera-Wasserberg concordia diagrams and age distribution plots for all analyzed spots of samples from Loc. 3 and Loc. 10 by LA-ICP-MS. The U–Pb ages of 28 zircon grains from the Loc. 10 sample show three peaks *ca.* 73, 85 and 105 Ma (Figure 10C). One Late Cretaceous, one Triassic and Two Proterozoic zircon grains also exist. The ages of 25 zircon grains from the Loc. 3 sample show three peaks *ca.* 70, 85 and 95 Ma (Figure 10D), and some older grains up to 420 Ma exist as well. The youngest age clusters for Loc. 10 and Loc. 3 are in the range 70–76 Ma and 68–75 Ma, and the weighted mean ages yield 73.0±1.8 Ma (MSWD = 1.7; 95% conf.) and 70.5±1.1 Ma (MSWD = 1.5; 95% conf.), respectively. These values are thought to indicate magmatism/deposition age of the tuff samples.

Discussion

Zircon geochronology reveals that the ages of the tuffs from the lowest and uppermost parts of the Etanpakku Formation in the Soya Hill area are 73.0±1.8 Ma and 70.5±1.1 Ma, respectively, which infer late Campanian to earliest middle Maastrichtian age.

The newly discovered ammonoid fauna from the Etanpakku Formation is characterized by *Gaudryceras izumiense*, which occurs frequently in the upper lower Maastrichtian in the Izumi Group of Southwest Japan and the Hakobuchi Formation in the Hobetsu area in south-central Hokkaido as well as the southern Talkeetna Mountains in southern Alaska (Matsumoto and Morozumi, 1980; Shigeta *et al*., 2010). According to Matsumoto and Morozumi (1980), the *Gaudryceras izumiense*-bearing beds (= *G. izumiense* Zone) include two distinct ammonoid faunas: *Pachydiscus kobayashii* (Shimizu, 1935), *Pachydiscus tanii* (Masumoto and Morozumi, 1980), *Nostoceras* aff. *hetonaiense* Matsumoto, 1977 and *Baculites regina* Obata and Matsumoto, 1963 in the lower part and *P*. aff. *flexuosus* Matsumoto, 1979, *P*. cf. *gracilis* Matsumoto, 1979 and *N*. aff. *kernense* (Anderson, 1958) in the upper part. Because the ammonoid fauna in the Soya Hill area includes *B*. *regina*, it is a correlative of the lower part of the *Gaudryceras izumiense* Zone of the upper lower Maastrichtian (Figure 11).

The *Gaudryceras izumiense* Zone, which is well

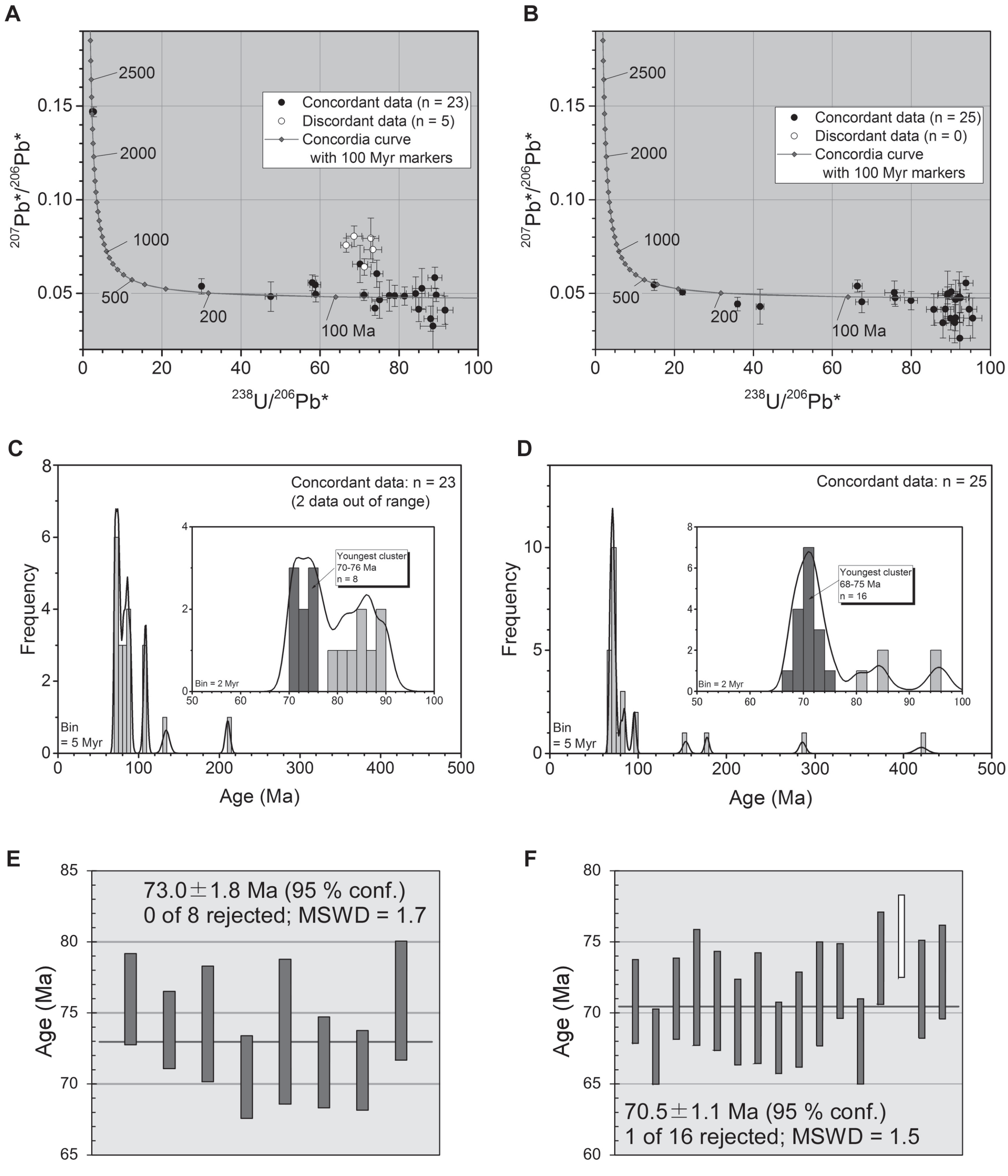

Figure 10. U-Pb zircon ages of tuff samples collected at Loc. 10 (**A, C, E**) and Loc. 3 (**B, D, F**). A, B, Tera-Wasserburg U–Pb concordia diagram of all data; C, D, Probability distribution diagrams of zircon ages (100 to 50 Ma); E, F, Age distribution plots of zircon ages in the youngest clusters. The uncertainties in the mean ^{238}U–$^{206}Pb^*$ ages represent 95% confidence intervals. $^{207}Pb^*$ and $^{206}Pb^*$ indicate radiometric ^{207}Pb and ^{206}Pb, respectively.

known in the upper part of Unit IVc of the Hakobuchi Formation in the Hobetsu area, contains *G. izumiense* as well as *Pachydiscus gracilis* and *P. kobayashii* (Matsumoto, 1979; Matsumoto and Toshimitsu, 1992; Shigeta *et al*., 2010). This fauna is probably identical to the upper part of the *Gaudryceras izumiense* Zone in the Izumi Group (Figure 11).

Because of the discontinuous occurrence of megafossils due to the predominance of coarse-grained sandstone, a complete succession of the *Gaudryceras izumiense* Zone is not recorded in the Hobetsu and Soya Hill areas. However, faunas in the *Gaudryceras*

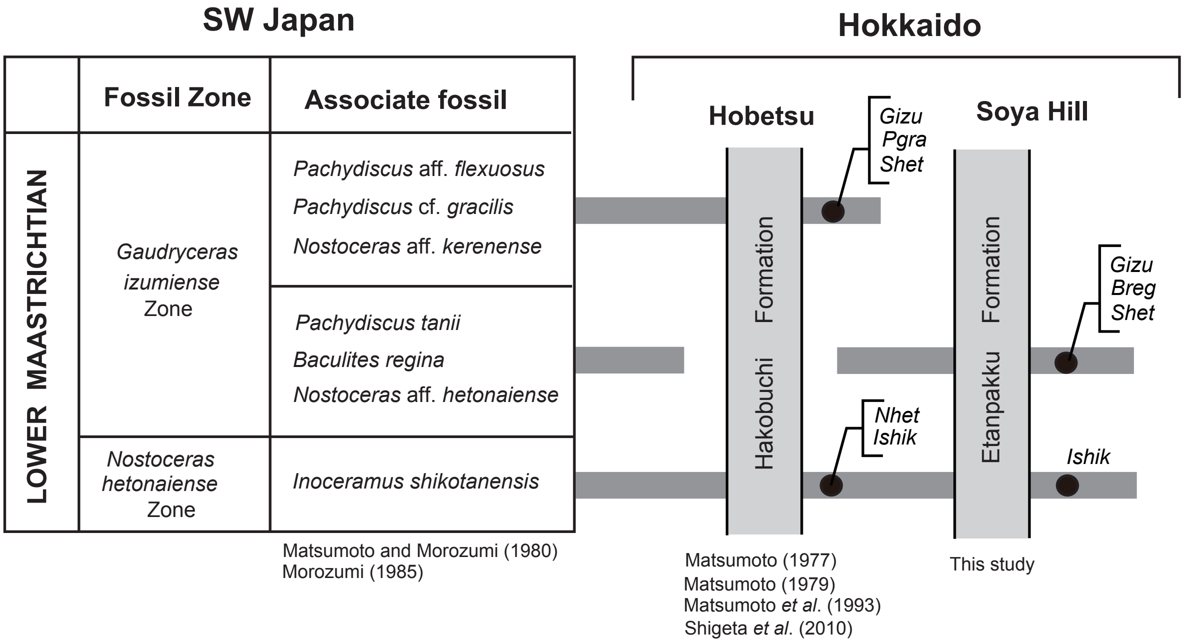

Figure 11. Diagram showing biostratigraphic correlation of the lower Maastrichtian in Southwest Japan (left) and Hokkaido (right). Breg, *Baculites regina*; Gizu, *Gaudryceras izumiense*; Ishik, *Inoceramus shikotanensis*; Nhet, *Nostoceras hetonaiense*; Pgra; *Pachydiscus gracilis*; Shet, *Sphenoceramus hetonaianus*.

izumiense Zone in Hokkaido suggest that similar faunas may have existed in the North Pacific realm during late early Maastrichtian time.

Paleontological description

Morphological terms are those used in Arkell (1957). Quantifiers used to describe the shape of ammonoid shell replicate those proposed by Matsumoto (1954, p. 246) and modified by Haggart (1989, table 8.1). All specimens were collected from the middle part of the Etanpakku Formation of the Yezo Group (= the *Gaudryceras izumiense* Zone of the upper lower Maastrichtian) exposed along the Onishibetsu and Sarukotsu rivers in the Soya Hill area.

Abbreviations for shell dimensionss.—*D* = shell diameter; *U* = umbilical diameter; *H* = whorl height; *W* = whorl width.

Institution abbreviations.—GK = Department of Earth and Planetary Sciences, Kyushu University, Fukuoka; HMG = Hobetsu Museum, Mukawa; NMNS = National Museum of Nature and Science, Tsukuba.

Suborder Phylloceratina Arkell, 1950
Superfamily Phylloceratoidea Zittel, 1884
Family Phylloceratidae Zittel, 1884
Subfamily Phylloceratinae Zittel, 1884
Genus ***Neophylloceras*** Shimizu, 1934

Type species.—*Ammonites* (*Scaphites*?) *ramosus* Meek, 1857.

Remarks.—*Neophylloceras*, established by Shimizu (1934, p. 61), has been regarded as either a synonym of *Hypophylloceras* Salfeld, 1924, a subgenus of *Hypophylloceras* or *Phylloceras* Suess, 1865, or as an independent genus (Murphy and Rodda, 2006). We herein follow the interpretation of Murphy and Rodda (2006).

Neophylloceras hetonaiense Matsumoto, 1942a
Figure 12

Neophylloceras hetonaiense Matsumoto, 1942a, p. 675, text-fig. 1; Spath, 1953, p. 5, pl. 1, fig. 2; Matsumoto, 1959, p. 5, pl. 3, fig. 1; Jones, 1963, p. 23, pl. 6, figs. 9, 10, pl. 7, figs. 1–5, text-fig. 12; Zonova *et al.*, 1993, p. 145, pl. 103, fig. 1; Yazykova, 1994, p. 288, pl. 1, figs. 5–7.

Neophylloceras lambertense Usher, 1952, p. 50, pl. 1, figs. 1–3.

Hypophylloceras (*Neophylloceras*) cf. *hetonaiense* Matsumoto. Matsumoto and Morozumi, 1980, p. 6, pl. 1, figs. 1–4.

non *Neophylloceras hetonaiense* Matsumoto. Matsumoto, 1984a, p. 11, pl. 1, figs. 4, 5; Matsumoto and Miyauchi, 1984, p. 38, pl. 10, fig. 1